

Orbiter-to-Orbiter Radio Occultation Measurements of Planetary Atmospheres and Ionospheres

J. V. HARRINGTON*

Center for Space Research, Massachusetts Institute of Technology, Cambridge, Mass.

AND

R. W. GOFF,[†] M. D. GROSSI,[‡] AND B. M. LANGWORTHY[§]

Raytheon Company, Bedford, Mass.

Profiles of the atmosphere and the ionosphere of a planet can be obtained on a global scale with an orbiter-to-orbiter radio occultation method when the two orbiters are used as terminals of a two-frequency RF probing link capable of providing integrated columnar measurements of the dispersive and nondispersive refractive properties of the medium along the propagation path. Analytical evidence shows that it is possible to obtain measurement accuracies of ± 500 el/cc for the atmospheric refractivity (with an additional 5% processing error incurred in the profile inversion). Spatial resolution with cell sizes of $600 \text{ km} \times 600 \text{ km} \times 1 \text{ km}$ is achievable and volumetric coverage of 90% of the atmosphere and ionosphere of a typical planet can be performed with an orbiting mission duration of approximately 180 days.

1. Introduction

THE plans formulated for planetary missions of the 70's include the simultaneous injection of pairs of orbiters around a planet. These configurations provide the opportunity of performing orbiter-to-orbiter radio occultation measurements that present specific advantages not found in orbiter-to-Earth occultation schemes.

In principle, all regions of the planet can be probed by this new scheme and repetitive refractivity measurements can be performed over any region to provide temporal variations on a global scale. Insensitivity to fluctuations in the refractive characteristics of the interplanetary medium which can affect single orbiter-to-Earth propagation paths is assured. Also, effects of the Earth's own ionosphere and atmosphere are eliminated.

The aim of the experiment is the measurement of the ionospheric and atmospheric refractivity from which the planet's atmospheric and ionospheric densities may be derived. The basic observables are the Doppler shifts affecting a two-frequency probing link established between the two orbiters. The dispersive and nondispersive Doppler components can be obtained by removing the range-rate Doppler from the total Doppler, and by resolving the residuals into atmospheric and ionospheric components.

Columnar refractivity measurements can then be converted to radial profiles. The conversion can be performed using the classical Abel transform, by model matching methods, or other inversion algorithms.

The columnar measurements are integral measurements, but they do resolve horizontal gradients on the scale to be expected in a planet's atmosphere and ionosphere. At surface level, measurable horizontal gradients span over a

range of a few degrees and therefore the method is able to resolve most of the expected day-side/night-side transitions.

Expected accuracies of the refractivity measurements are better than ± 500 el/cc for the ionospheric electron density (plus a 5% processing error incurred in the profile inversion) and better than ± 0.05 N-units for the atmospheric refractivity (plus, again, a 5% processing error).

Spatial resolution was chosen to have cell dimensions $600 \text{ km} \times 600 \text{ km} \times 1 \text{ km}$ height. These dimensions are the ones recommended by GARP (Global Atmospheric Research Program) for meteorological grids on Earth.¹

Typically, for a planet like Mars, volumetric coverage of 90% of the planet's atmosphere and ionosphere can be performed in 180 days; 45% in 90 days. The atmospheric and ionospheric refractivity data can be converted directly into electron density data and with the help of information on temperature and constituents obtained from other sources, neutral density profiles may also be derived.

2. Experiment Concept

The general dynamical geometry of the orbiter-to-orbiter scheme and the orbital parameters of the two vehicles must be chosen such that the line of sight between the two vehicles periodically sweeps through the planet's atmosphere first in a descending direction, then after cutting through the planet, emerges on the opposite side in an ascending direction. Radio signals between the orbiters propagate, therefore, through paths whose point of closest approach to the planet (offset point) alternately sweeps through near-vertical columns in the atmosphere and ionosphere. The region of interest for the probing experiment lies between the planet's surface and 1000 km altitude, a shell wherein all significant atmospheric and ionospheric phenomena occur. Thus, for each sweep through the planet, columnar refractivity measurements, taken in a manner to be described below, will provide a set of data which can be converted to a radial profile for the refractivity within the column.

The experiment requires a two-frequency, two-way phase-locked link between the first and the second orbiter. Typical frequency values for a Martian mission are 400 and 800 MHz. Each of the orbiters, by ground command, can function as "mother," initiating the probing operation with the radiated frequencies locked to the 2200 MHz DSN two-way link from Earth-to-mother. The second orbiter ("daugh-

Presented as Paper 69-53 at the AIAA 7th Aerospace Sciences Meeting, New York, January 20-22, 1969; submitted March 7, 1969; revision received September 9, 1969. This research activity has been sponsored by Raytheon Company, Equipment Division, Sudbury, Mass., as an Independent Research Project in the years 1965 to date. Additional support was obtained for the second half of 1967 from NASA-MSFC (Contract NAS 8-21222).

* Director, Associate Fellow AIAA.

[†] Celestial Mechanics Analyst.

[‡] Consulting scientist; also at Smithsonian Astrophysical Observatory, Cambridge, Mass. Member AIAA.

[§] Mathematician.

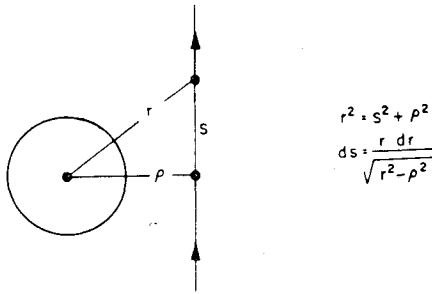


Fig. 1 Probing link geometry.

ter") is slaved to the phase of the signals received from the mother. The mother must be visible from the Earth while measurements are performed; the daughter may not.

Let us consider the case that both the mother and daughter are visible from Earth, but are not mutually visible. The mother is locked in phase with the Earth clock via the 2200 MHz DSN link, the daughter has the two VCO's (variable frequency oscillators) in the PLL (phase-locked loop) of the two-frequency transponder in "free-running" operation, but their frequency is monitored on Earth via the 2200 MHz link used as telemetry.

When eventually (because of the different orbital velocities) the radio visibility between the two orbiters is nearly established (situation of occultation "exit"), by ground adjustment the two probing frequencies radiated by the mother are moved to match the VCO frequencies in the daughter, and closed-loop operation between the two orbiters is established in a fraction of a second, with consequent acquisition of accurate data for the cells in the lower depths of the planet's atmosphere. Phase comparison between the signal provided by the daughter and the local Earth-locked reference is done on the mother and the data are then encoded and transmitted to Earth. Eventually, after the probing of a height span of the planet's envelope, the link reverses toward a new occultation event, and at "entry" the lower depths of the atmosphere again are probed with no loss of continuity in the phase lock between mother and daughter.

Let us now consider the case that only one orbiter is visible from Earth. This orbiter must then be chosen to be the mother; the second orbiter (daughter) again can be or not be within radio visibility with the mother. If it is, the operation is as follows: the mother is phase-locked to Earth, the daughter with the mother, and the mother transmits the experiment data to Earth until an event of occultation entry occurs. If it is not, at occultation exit probing starts again with degraded performances until mother-daughter phase lock is fully achieved. This "lock-in" time can be reduced by monitoring the VCO's of the daughter for the time interval in which this orbiter is in view of the Earth, with a procedure similar to the one described previously. The frequency of occurrence of this unfavorable condition is made negligible by appropriate choice of the orbits.

At each of the probing frequencies, f_1 and f_2 , the over all Doppler is characterized by the following components: 1) a geometric component (range rate) due to the relative motion of the two terminals; 2) a dispersive component due to propagation in the ionosphere; and 3) a nondispersive component due to propagation in the atmosphere. This component is indistinguishable from true range-rate Doppler. The latter rate must therefore be determined independently.

Once the Doppler residuals (total Doppler minus range-rate doppler) are obtained, the integration in the time domain provides the differential phase delays, $\Delta\phi$. We have

$$\Delta\phi(\rho)_{f-f_i} = \frac{f_i}{0.3} \left(\int_{-\infty}^{+\infty} [1 - \mu(r)] ds \right)$$

where f = frequency in MHz; r = radial distance in km;

$\mu(r)$ = index of refraction; s = path length in km; and ρ = distance from planet's center to ray's point of closest approach in km. The integration constant is zero because a free-space situation exists in the link's initial condition at entry, and final condition at exit.

With reference to Fig. 1, we can write by changing variables

$$\Delta\phi(\rho) = \frac{2f_i \times 10^{-6}}{0.3} \int_{\rho}^{\infty} \frac{N_i(r) r dr}{(r^2 - \rho^2)^{1/2}}$$

where r , ρ , and s are defined in Fig. 1 and $N_i(r)$ is the refractivity in N -units.

In the last equation the square root in the denominator is positive, because for every miss-distance ρ of the column from the center of the planet, $r > \rho$.

In order to obtain radial profiles, we have to perform profile inversion. One of the classical methods to do this is the Abel transform. Other methods belonging to the general category of model matching also may be employed.

By assuming to perform profile inversion by Abel transform, and by normalizing to the planet radius R_o , we obtain

$$N_i(r) = \frac{-3 \times 10^5}{\pi f_i r^2 R_o} \int_r^{\infty} \frac{\rho \Delta\phi(\rho) + \rho^2 \Delta\phi'(\rho)}{(\rho^2 - r^2)^{1/2}} d\rho$$

where now the square root in the denominator is positive because for every radial height r the refractivity is obtained from columnar measurements made at miss-distance ρ , always larger than r .

From the total refractivity profile, $N_i(r)$, measured at the frequencies f_1 and f_2 , electron density profile, $N_e(r)$, and atmospheric refractivity profile, $N_a(r)$, can be obtained as follows²

$$N_e(r) = 24,800 M_I(r) \times 10^{-6} \text{ el/cc}$$

$$N_a(r) = 3B_I/2 \times 10^{-6} [1 - B_I(r)]$$

where

$$M_I(r) = [N_1(r) - N_2(r)] / [(1/f_1^2) - (1/f_2^2)]$$

$$B_I(r) = \frac{2}{3} \times 10^{-6} \{N_1(r) - [M_I(r)/f_1^2]\}$$

This is done by assuming that on the planet the magnetic field is negligible and ionospheric refractivity therefore is solely a function of electron content, $N_e(r)$.

The interpretation of the atmospheric refractivity profile, $N_a(r)$, in terms of atmospheric parameters like pressure is more involved and requires the introduction of assumptions, or the utilization of measurements, which are not derived from the radio occultation experiment outcomes. A possible sequence of steps in this process is outlined in Ref. 3.

3. Orbital Mechanics Analysis

A preliminary orbital mechanics analysis of the mother/daughter radio occultation experiment has been formulated for a typical Martian mission. Realistic orbital parameters were selected for the two orbiters, and the resulting atmospheric probings as well as the pattern and extent of total planetary coverage were determined.

The following nominal orbital parameters were selected in order to examine the constraints imposed by the orbital geometry on the experiment results and the extent of planetary coverage provided by the scheme. The two orbiters were assumed to be inserted into Martian orbit at a time approximately equal to the time at which the sun's declination relative to the Martian equator reaches its maximum negative value ($\approx -24^\circ$).

The size of the mother's orbit was chosen with a 2000 km periapsis height and a 17,000 km apoapsis height. This corresponds to a semimajor axis (a_M) of 12,878 km and an orbital eccentricity (e_M) of 0.58239.

Table 1 Orbital parameters

Parameter	Mother	Daughter
a (semimajor axis)	12,878 km	13,097 km
e (eccentricity)	0.58239	0.58239
i (inclination)	60°	80°
ω (argument of perigee)	270°	270°
Ω (right ascension of ascending node)	0°	0°
θ (true anomaly)	0°	0°

The orbital size of the daughter was determined by increasing the major axis of the mother by the amount necessary to provide one 360° cycle of relative motion in approximately 20 days while maintaining the same orbital eccentricity (e_D) of 0.58239.

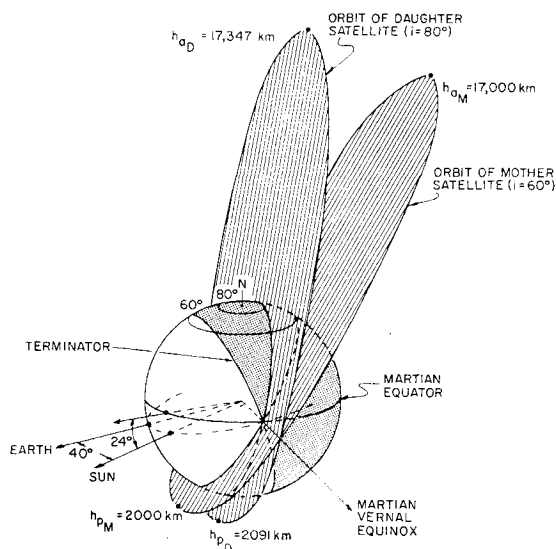
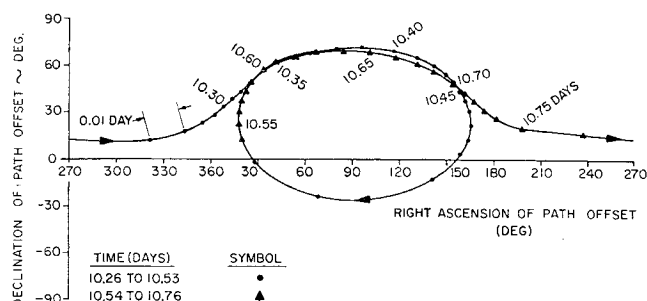
The orbital inclination of the mother was chosen as 60°. The range of possible orbital inclinations for the daughter was chosen between 50° and 80°. A daughter inclination of 80° was selected since this represented the maximum departure from the mother's orbit.

Orbits with relative inclinations of more than a few degrees are assumed to be established by dual launches or dual trans-Mars trajectories. In this way the relative orbital inclination is easily achieved (for the same trans-Mars injection energy) simply by changing the aiming point around the planet.

The fuel requirements become substantial when the relative inclination is established subsequent to the injection of the pair of satellites into Martian orbit. For the 20° relative inclination orbits cited, a velocity impulse of approximately 35% of the orbital velocity would be required.

The lines-of-nodes of both orbiters were chosen perpendicular to the Mars-Sun line with the ascending nodes coincident with the Martian Vernal Equinox at a mission time of 45 days. This minimizes the possibility of sun occultation. Periapsis was located at 270° from the ascending node in both cases. Figure 2 depicts the orbital geometry assumed. In this figure the ecliptic plane and the Martian orbital plane are shown coincident since their relative inclination is only 2°. Each orbiter was assumed to be at periapsis at the start of the mission. The orbital parameters assumed are summarized in Table 1.

Each phase path measurement made during the dual-orbiter occultation experiment is associated with the point along the geometric line-of-sight between mother and daughter that lies closest to the Martian surface. This point is referred to subsequently as the path offset point.

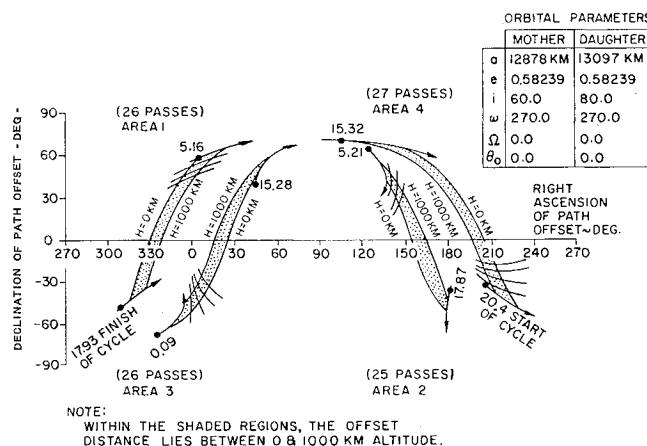
**Fig. 2 Assumed orbital geometry at $t = 45$ days.****Fig. 3 Typical ground trace of the path offset.**

The atmospheric volume probed depends upon the excursions made by the path offset point during the operating life of the experiment. These excursions depend upon the orbital parameters of the mother and daughter orbits. The coverage obtained by the orbits defined in Table 1 has been examined for the first 360° cycle of relative rotation which takes approximately 20 days to complete.

A typical history of the ground trace of the suboffset point during one revolution of the orbiting pair is shown beginning at 10.26 days from separation on the left-hand side of Fig. 3 and ending at 10.76 days on the right-hand side. During this revolution the altitude of the offset point makes two excursions from below the surface to approximately 1400 km and back.

Figure 4 shows the locus of the right ascension and declination of the ground trace of the offset point (referenced to the Martian Equator and Vernal Equinox) at times when the offset point is either at the planet surface or at an altitude of 1000 km. When the offset point lies within these regions, shown shaded on the figure and marked areas 1, 2, 3, and 4, the actual probing experiment is conducted. The exact path and direction of the ground traces through these areas are indicated for the first few coverage passes in each area with the direction of motion shown by the arrow. The horizontal ground distance traversed while the offset point moves vertically between 0 and 1000 km altitude is approximately 600 km.

The coverage cycle shown was assumed to begin with the mother and daughter orbiters at their periapsides. Several days are required before the mother, which lies in a somewhat lower orbit, moves sufficiently far ahead of the daughter such that the offset point decays to the surface during a revolution of the pair. Therefore, occultation measurements actually begin in area 4 at 2.04 days and continue to area 3 at 2.09 days. A total of 27 passes in area 4 and 26 in area 3 will be made, each pass in an area being separated in time by one orbital period (approximately 12 hr). The sequence

**Fig. 4 Dual orbiter occultation experiment coverage during first data collection cycle. (Vertical axis represents declination of path offset measured in degrees.)**

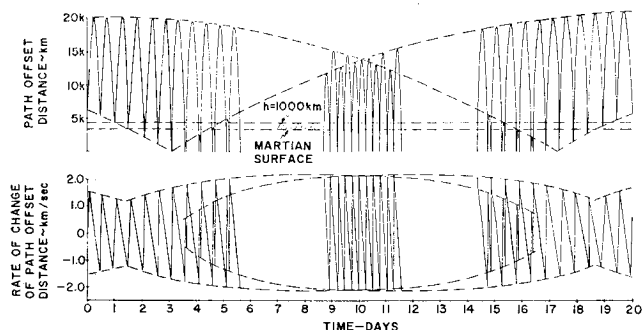


Fig. 5 Path offset distance and rate of change.

between areas 4 and 3 continues for 7 passes through area 4 and 6 through area 3 at which time coverage in two new areas is added, beginning at 5.16 days in area 1 and 5.21 days in area 2. The path offset moves through areas 1, 2, 3, and 4 until 15.32 days when areas 3 and 4 disappear and coverage is obtained in areas 1 and 2 only. Coverage in areas 1 and 2 continues until 17.87 days when measurements in this cycle are terminated. At this time the mother has moved ahead of the daughter by almost one complete revolution. At 20 days the two orbiters are approximately together at their corresponding periapsides, marking the end of one complete cycle of relative motion. A second coverage cycle similar to the first would begin at 22 days.

The time variation of the path offset distance and its rate of change over one cycle is shown in Fig. 5. Experimental measurements occur during the times when the path offset distance ranges between 3378 km (the radius of Mars) and 4378 km (1000 km altitude). This region is shown shaded in this figure. Note, that beginning at 5.16 days, four passes through the altitude band per 12 hr orbital period are obtained. This point was shown in Fig. 4 and corresponds to the offset point moving from one side of the planet to the other side due to the relative motion of the orbiters, as first one then the other passes through periapsis. At this time, the experiment transmitter duty cycle places the severest drain requirement on battery energy since four passes occur within approximately $4\frac{1}{2}$ hr.

When the offset point lies between 0 and 1000 km altitude, the nominal rate of change is ± 1 km/sec. This dictates a measurement sampling time of 1 sec since a resolution cell of 1 km in height has been taken as a scientific goal in this experiment.

The time variation of the range and range-rate between mother and daughter over one cycle is shown in Fig. 6. The maximum range of 25,800 km occurs at midcycle when one orbiter is at apoapsis while the other is at periapsis. The range rate between the orbiters varies between roughly ± 1 km/sec during the entire cycle. This figure is used to provide an estimate of the maximum geometric Doppler to be expected during the experiment.

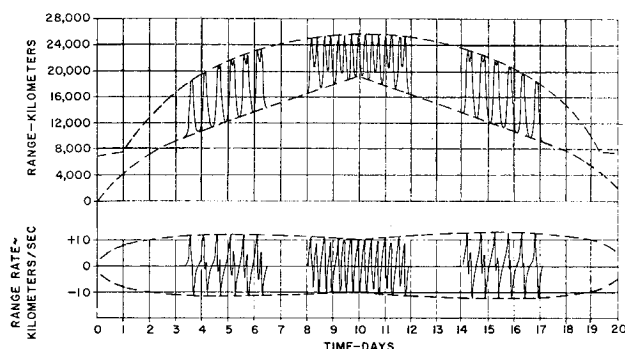


Fig. 6 Orbiter-to-orbiter range and range rate.

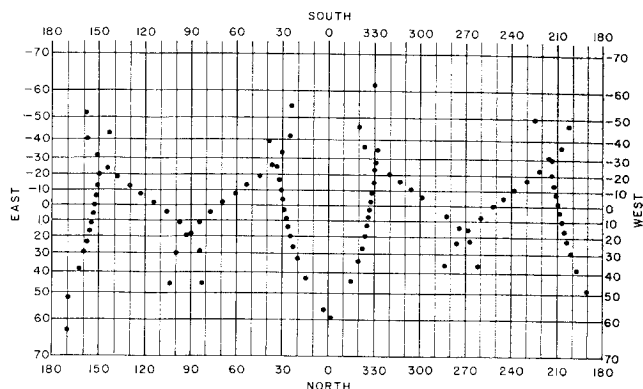


Fig. 7 Dual orbiter occultation experiment coverage during first data collection cycle (20 days)—Mars coordinate system.

The complete sampling of the time-dependent characteristics of the atmosphere would require offset point measurements at various latitudes and longitudes with respect to the sun, at various times of year and at various levels of solar activity. Since the total duration of the experiment has been chosen to be nominally 90 days, the latter effect, which is expected to cause a density variation of three orders of magnitude at 1000 km altitude between regions of low- and high-solar activity, must remain undetermined. Extension of the measurements beyond the 90-day mission period can, however, yield some data on the effects of changes in solar activity. The degree to which this can be done successfully depends entirely on how much the mission is prolonged.

Because of its duration, the experiment is better suited for determining the diurnal (day-night) variations in the atmosphere of Mars corresponding to a value of solar activity that is estimated to lie midway between minimum and maximum. The magnitude of the diurnal density variation is estimated to be an order of magnitude at 1000 km altitude. For the ionosphere, variations of many orders of magnitude are expected.

In order to determine the diurnal effects at a given level of solar activity, samples must be taken for all altitudes from 0 to 1000 km at various latitudes and longitudes with respect to the maximum point of the atmospheric bulge. The bulge is assumed to be located at the latitude of the subsolar point, but is assumed to lag it by approximately 30° in longitude.

Because of the inclination of the orbits investigated, $i_D = 80^\circ$ and $i_M = 60^\circ$, the offset point covers the declination range from approximately -50° to $+60^\circ$. This declination

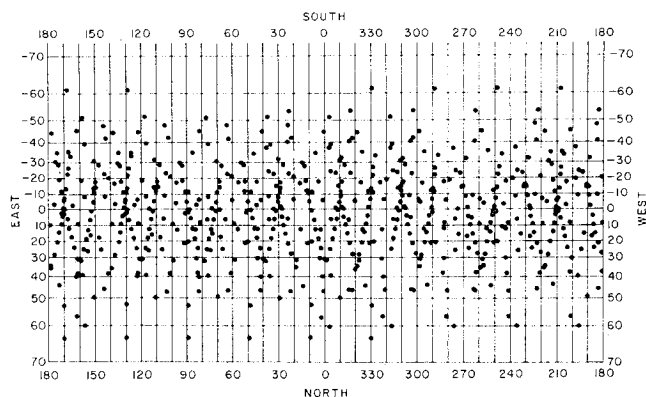


Fig. 8 Dual orbiter occultation experiment coverage during 120-day mission—Mars coordinate system.

Table 2 Errors in ionospheric electron density profile and atmospheric refractivity profile ($f_1 = 400$ MHz and $f_2 = 300$ MHz)

r Height (km)	$N_1(r)$		Absolute error in calculating $N_1(r)$	Absolute error in calculating $N_2(r)$	Resulting errors in calculation	
	$\epsilon^a = 0.009$ cycles	$N_2(r)$ $\epsilon = 0.018$ cycles			$N_e(r) \pm \Delta N_e(r)_{\max}$ (el/cc)	$N_a(r) \pm \Delta N_a(r)_{\max}$ (el/cc)
0	3.478	3.466	0.007	0.002	62 \pm 173	3.462 \pm 0.01
5	2.441	2.429	0.031	0.004	66 \pm 466	2.425 \pm 0.03
10	1.642	1.620	0.006	0.002	120 \pm 74	1.612 \pm 0.00
20	0.786	0.760	0.019	0.012	133 \pm 131	0.752 \pm 0.01
30	0.362	0.330	0.079	0.020	167 \pm 187	0.320 \pm 0.01
40	0.175	0.134	0.098	0.045	215 \pm 124	0.121 \pm 0.01
50	0.120	0.062	0.096	0.016	304 \pm 67	0.043 \pm 0.00
60	0.127	0.045	0.009	0.228	437 \pm 60	0.017 \pm 0.01
70	0.186	0.050	0.031	0.144	717 \pm 69	0.005 \pm 0.01
80	0.347	0.094	0.037	0.267	1335 \pm 202	0.010 \pm 0.03
90	0.879	0.234	0.000	0.013	3412 \pm 21	0.019 \pm 0.00
100	-2.461	-0.632	0.001	0.007	9679 \pm 40	-0.022 \pm 0.00
110	-15.328	-3.937	0.000	0.009	60207 \pm 192	-0.140 \pm 0.04
115	-22.328	-5.541	0.001	0.004	88815 \pm 299	0.054 \pm 0.04
120	-25.409	-6.297	0.002	0.001	101117 \pm 343	0.073 \pm 0.03
125	-24.778	-6.267	0.000	0.001	97933 \pm 87	-0.097 \pm 0.01
130	-22.697	-5.701	0.000	0.000	89917 \pm 36	-0.036 \pm 0.00
140	-16.475	-4.142	0.001	0.001	65228 \pm 149	-0.036 \pm 0.01
150	-11.058	-2.776	0.000	0.001	43816 \pm 56	-0.016 \pm 0.00
160	-7.179	-1.800	0.002	0.001	28460 \pm 103	-0.007 \pm 0.00
170	-4.580	-1.147	0.001	0.002	18166 \pm 55	-0.002 \pm 0.00
180	-2.738	-0.685	0.005	0.007	10860 \pm 107	-0.001 \pm 0.01
200	-1.083	-0.270	0.003	0.028	4297 \pm 58	-0.000 \pm 0.01
225	-0.580	-0.145	0.002	0.052	2304 \pm 46	0 \pm 0.01

^a ϵ = phase error.

band contains 81.5% of the total surface area of Mars. The coverage obtained in this region has been examined for the proposed dual-orbiter occultation experiment.

The volume between $+60^\circ$ and -50° latitude has been separated into resolution verticals that are $10^\circ \times 10^\circ$ in longitude and latitude (600 km \times 600 km at the equator) and extend from the surface to 1000 km altitude. In area 4 of Fig. 4 the first data collection cycle yields 11 columns with 27 passes through this area. In a 20-day cycle, therefore, the total number of verticals that can be sampled is 41. Out of a total of 396, this corresponds to 10% coverage of the Martian envelope.

The coverage areas during the second 20-day cycle (mission time 20 to 40 days) remain approximately the same as shown, since the offset point probes the same volume in inertial space, except for small changes in the orbits caused by planet oblateness which amount to 1) $\Delta\Omega$ (change in right ascension of the ascending node): mother, $-0.166^\circ/\text{day}$; daughter, $-0.054^\circ/\text{day}$; and 2) $\Delta\omega$ (change in argument of periapsis): mother, $+0.041^\circ/\text{day}$; daughter, $-0.133^\circ/\text{day}$.

During a 20-day period, the lines-of-apsides and the lines-of-nodes will stay within 3° of their original locations. However, the sidereal mean daily motion of the sun is 0.524° and, therefore, at the start of the second 20-day cycle, the data will differ in right ascension (relative to the sun) by $0.524^\circ \times 20 = 10.5^\circ$. This is approximately equal in width to a resolution vertical, indicating that each subsequent cycle will measure verticals that are shifted approximately one cell in right ascension relative to the sun.

Therefore, each cycle adds 41 new columns of information, and in 90 days, $90/20 \times 10\%$ or 45% coverage of the planet will be obtained between the $+60^\circ$ and -50° latitude band. If the mission duration is extended to 180 days, 90% coverage will be obtained.

The trace of the grazing point on the planetary surface in Mars coordinates showing the location at which vertical refractivity profiles would be taken during mission lifetimes of 20 and 120 days are shown in Figs. 7 and 8. The widespread coverage in longitude and the rather good coverage obtained at midlatitude are readily apparent.

Table 3 Instrumentation performance parameters

Symbol		400 MHz	800 MHz
f	Frequency	400 MHz	800 MHz
P_T	Transmitter power	43 dbm	47 dbm
G^2	Antenna gain (2-way)	0 db	0 db
L_P	Path loss (17,000 km)	172 db	175 db
T_c	Cosmic noise temperature	100°K	50°K
F	Noise figure	5 db	6 db
L	Coax losses	1 db	1 db
T_e	Total effective noise temperature	900°K	1100°K
	Noise power/Hz	-169 dbm/Hz	-168 dbm/Hz
	Noise power-45 KHz BW	-122.5 dbm	-121.5 dbm
P_R	Received power	-130 dbm	-129 dbm
	S/N-45 KHz BW	-715 db	-7.5 db
	MIN S/N-45 KHz BW ^a	-20 db	-19 db
	S/N-100 Hz	19 db	19 db
	Estimated S/N degraded performance ^b	10 db	10 db

^a MIN S/N required to assure detection and one hour mean time to lock.^b Includes fading, antenna, and component degradation.

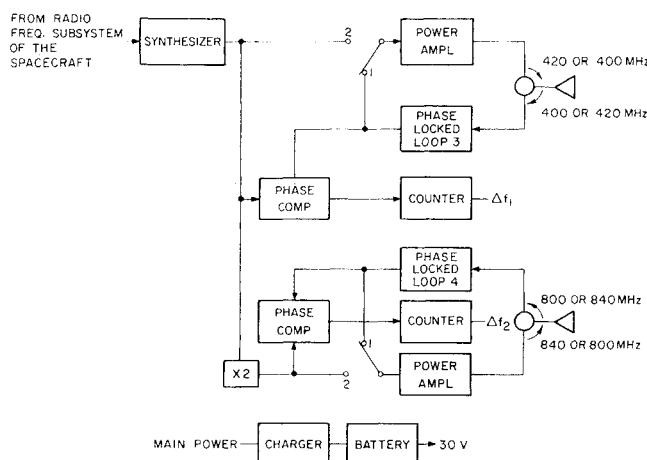


Fig. 9 Instrumentation block diagram at each orbiting terminal. (Switches in "transponder" position.)

4. Measurement Accuracy and Instrumentation Performance Parameters

Table 2 shows that the accuracy goals of the experiment set in Sec. 1 can be met with an instrumentation capable of performing phase measurements with standard deviation of 0.009 cycles at 400 MHz and 0.018 cycles at 800 MHz.

These requirements translate in the instrumentation performance parameters listed in Table 3 and in range rate rms error requirements of 0.020 cm/sec, which is within the present state-of-the-art.

Positional requirements are not very stringent and well within the present capability of Deep Space Network (DSN).

The over-all instrumentation block diagram is shown in Fig. 9. Operation is shown with the control switch in position 1, which represents the conditions whereby signals originate in Orbiter I with Orbiter II being merely a transponder. The converse is possible when control switches are in position 2. This will permit operation when either orbiter is occulted from Earth and also will provide redundancy for increased reliability.

The system requires a highly stable signal in order to make the phase measurements to the desired accuracy. Phase errors of 0.035 Hz in a 100 Hz bandwidth require stabilities of $1/10^7$ /sec. It is felt therefore that operation with a phase locked to the S-band frequency transmitted from Earth to the orbiter (stability $1/10^{12}$ /sec) is desirable. This will permit refractivity measurements to be made to the desired accuracy at all times that one of the two orbiters is visible from Earth.

Table 4 presents the summary of the weight, size, and power consumption values that characterize the instrumentation.

Table 4 Summary of equipment characteristics

	Weight, lb	Size, in.	Peak power, w	Avg power, w
Transmitter				
phase locked loop	1	10 × 2.5 × 2.5	1	0.1
400 MHz Ampl	1	10 × 1 × 0.5	40	1.6
800 MHz Ampl	3	10 × 1 × 2	120	4.8
Receiver				
phase locked loop				
(2)	2	10 × 2.5 × 5	2	0.1
phase detector and				
counter (2)	1	10 × 2.5 × 2	1.5	0.1
Batteries	6	10 × 2.5 × 5
Antennas	1
Totals	15	10 × 12 × 5	164.5	6.7

5. Conclusions

The previous sections have shown that an instrumentation package with limited weight, size, and primary power requirements installed in each one of the two orbiters makes possible the performance of a radio occultation experiment that eliminates all the problems attendant to these measurement schemes. Prior to the space age, occultation methods were limited to Earth-based observations⁴ of the absorption and refractive effects imposed by these media upon the electromagnetic radiation from a chosen star.⁵⁻⁸

Problem areas were the following: 1) poor signal-to-noise ratio; 2) rarity of usable occultations; 3) small ratio of the scale height of the planet's atmosphere to the planet/Earth distance. This causes sizable signal attenuation; 4) probing confined to the upper layer of the atmosphere under investigation; 5) decrease in measurement accuracy due to the effects of the Earth's own atmosphere and ionosphere; 6) limitation of the probing to only two regions in the planet's atmosphere; 7) nonrepetitive measurements; and 8) sensitivity to sudden change in the refractivity and absorptive characteristics of the interplanetary medium.

The development of space technology has made possible significant improvements of the scheme that have removed many of its limitations.⁹

Even in the case of a single space platform, two new concepts emerge. One concept involves a transmitter installed in the space platform that either orbits or flies by a planet using a detector installed on the Earth's surface. The Mariner IV radio occultation experiment¹⁰ is the pioneering experiment using this concept wherein the space vehicle flew past a target planet. This concept eliminated all the problems previously discussed with the traditional occultation experiments, except problems 5, 6, 7, and 8. If the space vehicles had been an orbiter, problem 7 also would have been eliminated. An example of this configuration, but with the sun in place of the planet, is the Massachusetts Institute of Technology Sunblazer experiment, which probes the solar atmosphere.¹¹

The second concept uses a star or the Sun as the radiator of electromagnetic energy whereas the detector is installed in an orbiting or flyby spacecraft. This concept already has been used in the following satellite missions:

1) NRL-1964-01-D and NRL-1965-16-D Satellites which measured the density of the Earth's upper atmosphere from the attenuation of the solar x-rays (44-60 8-14, 8-12 Å) taking place along the line of sight between the satellite and the sun, while this line was descending through the Earth's upper atmosphere at the occultation entry and exit.¹²

2) OSO III Satellite, which in March 1967 measured the upper atmospheric density of the Earth from the attenuation of the 630 Å and 430 Å sun radiation while again the line of sight, sun-to-satellite, was cutting through the Earth's

atmosphere.¹³ This concept eliminated all the problems of the traditional experiments except those identified as problems 6, 7, and 8. If an orbiter is used, problem 7 vanishes.

When two space platforms are available, it is possible to replace the natural noncoherent electromagnetic source with a coherent transmitter and, at the same time, substitute the Earth-bound detector with a receiver also placed in the vicinity of the planet under study.

The dual flyby scheme¹⁴ belongs to this category. This configuration provides significant advantages. However, problems 6 and 7 of the traditional experiment still remain unsolved, since only two regions of the planet's atmosphere are probed and the measurements are not repetitive.

All limitations are eliminated if both space platforms orbit the planet. Thus, the orbiter-to-orbiter configuration appears to be the most suitable for occultation experiments to probe the atmosphere and ionosphere of the planets, and the opportunity provided by dual-orbiter missions of the 70's should not be missed.

References

¹ Report on the Study Conference ICSU/IUGG, Stockholm, Sweden, June 28–July 11, 1967.

² "Electromagnetic Probing of the Mars and Venus Atmospheres and Ionospheres from an Orbiting Pair," Final Rept., Contract NASW-1772, Sept. 1969, Raytheon Co., Sudbury, Mass.

³ Harrington, J. V., Grossi, M. D., and Langworthy, B. M., "Mars Mariner 4 Radio Occultation Experiment: Comments on the Uniqueness of the Results," *Journal of Geophysical Research, Space Physics*, Vol. 73, No. 9, May 1968, pp. 3039–3041.

⁴ Weisberg, H. L., "The Study of Planetary Atmospheres by Stellar Occultation," Rept. RM-3279-JPL, Oct. 1962, Rand Corp.

⁵ Baum, W. A. and Code, A. D., "A Photometric Observation of the Occultation of Sigma Arietis by Jupiter," *Astronomical Journal*, Vol. 58, 1953, pp. 108–112.

⁶ Menzel, D. H. and DeVancouleurs, G., "Results from the Occultation of Regulus by Venus," *Astronomical Journal*, Vol. 65, 1960, p. 35.

⁷ Elsmore, B., "Radio Observations of the Lunar Ionosphere," *Philosophical Magazine*, 1957, p. 1040.

⁸ Vitkevich, V. V., "New Method of Investigating the Solar Corona," *Doklady Akademii Nauk SSSR*, Vol. 77, No. 4, 1951, pp. 585–588.

⁹ Weisberg, H., "On the Possibility of Studying Planetary Atmospheres by Observing Stellar Occultations from a Flyby Space Probe or Planetary Orbiter," *Icarus*, Vol. 2, 1963, pp. 226–227.

¹⁰ Kliore, A. et al., "Occultation Experiment: Results of the First Direct Measurement of Mars' Atmosphere and Ionosphere," *Science*, Vol. 149, 1965.

¹¹ Harrington, J. V., "Study of a Small Solar Probe (Sunblazer) Part I, Radio Propagation Experiment," MIT Rept. PR-5255-5, July 1965, Massachusetts Institute of Technology.

¹² Landini, M. et al., "Atmospheric Density in the 120–190 km Region Derived from the X-Ray Extinction Measured by the US NRL Satellite-1964-01-D," *Nature*, Vol. 206, 1965, pp. 173–174.

¹³ Hinterregger, H. E., private communication, Air Force Cambridge Research Labs., Bedford, Mass.

¹⁴ Coogan, J. M., "A Method for Studying Planetary Atmospheres Employing the Dual Flyby Mode," *AIAA Journal*, Vol. 5, No. 6, June 1968, pp. 625–632.